Microfluidization of Ginger Rhizome (Zingiber officinale Roscoe) Juice: Impact of Pressure and Cycles on Physicochemical Attributes, Antioxidant, Microbial, and Enzymatic Activity

Microfluidization of Ginger Rhizome (*Zingiber Officinale Roscoe*) Juice: Impact of Pressure and Cycles on Physico-chemical Attributes, Antioxidant, Microbial and Enzymatic Activity

Rajat Suhag[1], Shivam Singh[2], Yogesh Kumar[3], Pramod K Prabhakar[2] & Murlidhar Meghwal[2]*

[1]Faculty of Agricultural, Environmental and Food Sciences, Free University of Bozen-Bolzano, Italy

[2]Department of Food Science and Technology, National Institute of Food Technology Entrepreneurship and Management, Sonipat-131028, Haryana, India

[3]Department of Agricultural and Food Sciences, University of Bologna, Piazza Goidanich 60, 47521, Cesena, FC, Italy

[*]**Corresponding author**

Murlidhar Meghwal

Department of Food Science and Technology, National Institute of Food Tech Technology Entrepreneurship and Management, Sonipat-131028, Haryana, India

Email: murli.murthi@gmail.com

Abstract

The aim of this study was to investigate the effects of high-pressure microfluidization on the physico-chemical attributes, antioxidant, enzymatic and microbiological activity of ginger rhizome (*Zingiber officinale Roscoe*) juice at different microfluidization pressures (68.94, 103.42, and 137.89 MPa) and cycles (1, 2, and 3). An important physical attribute, the mean particle size of ginger rhizome juice, was significantly ($p<0.05$) decreased from 15.85 (control) to 12.86 µm at 137.89 MPa and 1 cycle, which was further supported by microscopic inspection revealing cell disintegration. Due to the release of phenolic compounds and pigments brought on by cell disruption, total phenolic content, antioxidant activity assays DPPH, and ABTS values increased from 56.79 to 65.28 mg GAE/100 mL, 69.99 to 77.51% inhibition and 74.61 to 84.74% inhibition, respectively, at 103.42 MPa and 3 cycles. The polyphenol oxidase (PPO) enzyme was shown to be baroresistant because microfluidization had no noticeable impact on its relative activity. A higher microfluidization pressure of 137.89 MPa resulted in the complete reduction of aerobic bacteria, yeast, and molds. Due to its solvent-free nature and success in microbial reduction, microfluidization may aid in the delivery of high quality clean-labelled ginger juice. The findings demonstrated that microfluidization treatment has the potential to produce clean-label, safe ginger juice with improved overall quality. This study provides useful information to industries for the commercialization of ginger juice and will assist in promoting the usage of undervalued rhizome species.

Keywords: Ginger; Novel processing; Antioxidant activity; Microbial safety; Juices.

1 Introduction

Ginger rhizome (*Zingiber officinale Roscoe*) is a popular spice known for its wide spectrum of therapeutic properties. It contains carbohydrates (60–70%), crude fiber (3–8%), protein (9%), ash (8%), fatty oil (3–6%) and volatile oil (2–3%). The characteristic flavor of ginger is due to zingerone, shogaols, gingerols, and volatile (essential) oils, which constitute up to 3% of ginger on fresh weight basis (Ali et al. 2008). The composition of volatile and non-volatile components in ginger varies depending on the species and climatic conditions. The volatile fragrant essential oil of ginger contains mainly sesquiterpenoids, with α-zingiberene (30–70%) being the main component, along with smaller amounts of other sesquiterpenoids: β-sesquiphellandrene (15–20%), β-bisabolene

(10–15%), and α-farnesene, and monoterpenoids (β-phellandrene, camphene, cineol, geraniol, citral, etc.). Ginger also contains diterpenes and ginger glycolipids (Ali et al. 2008; Srinivasan 2017). Gingerol, shogaol, paradol and zingerone (F. Chen et al., 2019; Shukla et al., 2019) are the key phytochemicals found in the ginger rhizome which are accountable for different therapeutic properties, i.e. antioxidant, anti-inflammatory, neuroprotective, protective effects against respiratory disorders, hepatoprotective, antiviral, anti-fungal, anti-parasitic, immunomodulatory, gastrointestinal activity, anti-arthritic, hypoglycemic activity, anti-ulcer and relief in constipation and flatulence (Ban et al., 2020). The abundance of phytochemicals contributes to the increased consumption of ginger in daily life. It is consumed in different forms of products, including beverages, confectionery, bakery and health supplement products. For example, ginger juice is used as a flavoring component in ice cream (Gabbi et al. 2018; Pinto et al. 2009). The addition of ginger rhizome juice to ice cream reduced the total solids, fat and protein content, and overrun, while increased the antioxidant activity, total phenols and melting resistance (Gabbi et al. 2018). Furthermore, it has been used in a ready-to-serve (RTS) herbal beverage (K Gaikwad 2012), yoghurt (Zhong et al. 2017) and Sandesh (Bandyopadhyay et al. 2008).

From a safety standpoint, thermal processing is a commonly used technique to inactivate natural enzymes and detrimental microbes. However, when spices like ginger are exposed to high temperatures, they lose their vital volatile components (D. Chen et al. 2016). Also, thermal processing has detrimental effects on the color, taste, and nutrients of processed food products (Chakraborty et al. 2016). Non-thermal processing techniques, like high pressure processing, high-energy pulsed electric fields and high pressure carbon dioxide, have been used to inactivate the PPO enzyme and preserve the color of carrot juice (Koley et al. 2020a) and cloudy ginger juice (D. Chen et al. 2016). Similarly, the application of high pressure microfluidization as a non-thermal technique has intensified recently because of the flexibility of microfluidizers in processing conditions, as both pressure and cycles can be optimized to specific requirements (Dhiman and Prabhakar 2021). Microfluidization is a novel technique that includes slamming liquid-liquid or solid-liquid structures together at high velocity and strong shear (Kumar et al. 2022). This is achieved by splitting a pressurized liquid stream and directing it toward one another so that they collide head-on in an interaction chamber (Suhag et al. 2022). Because of the collision and the high pressure in the interaction chamber, shear and impact forces arise, resulting in particle size reduction, cellular disruption, and structural alterations of food components (e.g. proteins and carbohydrates) (Bitik et al. 2019; Mert et al. 2014a; Suhag et al. 2021).

Microfluidization has recently piqued the interest of researchers and industries due to a number of advantages: (i) it is a green technology because it does not use any chemicals or solvents during processing; (ii) it produces smaller and more uniform particle sizes; (iii) less processing time, therefore, reduced processing costs; (iv) very few to no chances of contamination during processing; (v) easy scalability from small-batch processes to continuous processing; (vi) there are no moving parts in the equipment, which increases its lifespan; and (vii) produces highly consistent and reproducible results under the same operating parameters and conditions. Microfluidization has mostly been used for the development of emulsions, such as pea globulin-based emulsion (Oliete et al. 2019), olive oil-in-water pickering emulsion (Espinosa-Solís et al. 2021), gel-like emulsion with whey protein isolate (Y. Liu et al. 2019), nanoemulsion containing natural antibacterial mixture of citral, trans-2-hexen-1-ol, and linalool (1:1:1 w/w) (Taghavi et al. 2018), double (water-in-oil-in-water) emulsion to carry hydrophilic (chlorophyllin) and/or hydrophobic (lemongrass essential oil) active compounds (Artiga-Artigas et al. 2019) and rutin loaded oil-in-water emulsion (Dammak and do Amaral Sobral 2017). Furthermore, it has also been used for the modification of legume (chickpea and lentil) starch (Bitik et al. 2019) and as a milling process for wheat bran fibers to be used as an functional ingredient in bakery products (Mert et al. 2014b).

Certain juices have been microfluidized at different pressure-cycle combinations, which has shown significant changes in the physico-chemical, functional, microbial and enzymatic properties of microfluidized juices, however the results vary from juice to juice. Koley et al., (2020b) observed an increase in the carotenoid content of microfluidized carrot juice, but no clear trends for antioxidant activity and total phenolic content. Karacam et al., (2015) on microfluidizing strawberry juice reported that low pressure (60 MPa) had no significant effect, whereas, high pressure (100 MPa) lead to an increase of 22% in antioxidant activity. Tarafdar et al. (2019) also showed an increase in the total phenolic content, total flavonoid content and free radical scavenging activity of sugarcane juice microfluidized at 120 MPa as opposed to a reduction at pressure of 100 MPa and 140 MPa. Furthermore, a recent study by Ke et al. (2022) treated whole mango juice using an industrial scale microfluidizer and demonstrated that it lead an improvement in the antioxidant activity. In the case of micronizing mushrooms and P. *pyrifolia* (Chinese pear) juice, Liu et al., (2009) found that PPO was not inactivated, in contrast to the treatment of pressure and number of cycles that increased the relative activity of PPO. On the contrary, Tarafdar, Kaur, et al. (2021) reported a reduction of 39.4-64.7% in the PPO activity upon microfluidization of sugarcane juice, but complete inactivation was not achieved.

According to Grand View Research, (2022) report, fruit juices held the largest market share in the global juice industry in 2021, representing 61.2% of the total global revenue. Furthermore, the majority of studies described above focused on the microfluidization of fruit juice and a few vegetable juice. D. Chen et al. (2016) reported that the high hydrostatic pressure (500 MPa, 10 min) was better treatment compared to ultrahigh temperature (110 °C for 8.6 s) for keeping quality of cloudy ginger juice. This study only reported the results of one pressure level (500 MPa), during which there was an increase in temperature of 18 °C (from 20 to 38 °C), which may be detrimental due to the longer holding time of 10 min in high hydrostatic pressure. As a result, high pressure microfluidization that has a residence time of 1-5 milliseconds inside the interaction chamber (velocities up to 500 m/s) (Microfluidics chamber user guide 2015) may be a viable alternative for processing ginger juice. In addition, there is very limited research on the effects of microfluidization, which is being explored in this study to investigate ginger juice. In this study, the authors aims to determine the resulting changes by microfluidization on physico-chemical properties and antioxidant, enzymatic, and microbial activity of ginger juice at different pressures and cycle combinations. The findings demonstrated that microfluidization treatment has the potential to produce clean-label, safe ginger juice with improved overall quality. This study provides useful information to industries for the commercialization of ginger juice and will assist promote the usage of undervalued rhizome species.

2 Materials and methods

2.1 Materials

Freshly harvested ginger rhizomes (*Zingiber officinale Roscoe*) were bought (in November 2022) from a local market in Kundli, Haryana, India. Folin-Ciocalteu reagent, 1,1-diphenyl-2-picrylhydrazyl (DPPH), 2,2'-azino-bis(3-ethylbenzothiazoline-6-sulfonic acid (ABTS), gallic acid, sodium carbonate, potassium persulfate, methanol, ethanol, phosphate and catechol were purchased from Sigma Aldrich, India. Whereas, plate count, peptone water and potato dextrose agar were bought from HIMEDIA, India. All other reagents were of analytical grade.

2.2 Ginger juice extraction

Ginger rhizomes were manually sorted, graded, and cleaned before being peeled off with a stainless steel peeler. Ginger was then subjected to a juicer (Bajaj JEX 16, India) to extract the juice, which was later filtered using a four-fold muslin cloth as ginger juice is rich in fiber content. Traces of non-soluble fiber in the juice may clog the microchannels of the microfluidizer. After filtration, the amount of juice extracted was measure and noted in liters

(L). Additionally, to determine the density of juice, a 50 mL empty measuring cylinder was placed on a weighing balance (Sartorius AG Germany), and its weight was tared. The measuring cylinder was filled with 50 mL of juice, and its weight (in g) was noted.

2.3 Microfluidization treatment

Ginger juice (200 mL) was microfluidized through an electric benchtop lab scale microfluidizer (M-110P, Microfluidics Corp., MA, USA) equipped with a diamond fixed Y-type geometry (F12Y) interaction chamber (75 µm pore size), followed by an auxiliary processing module (APM) for fluid flow stabilization. Three microfluidizer pressure levels: 68.94, 103.42 and 137.89 MPa, with three different numbers of cycles: 1, 2 and 3, were applied to the ginger juice. Following each treatment, the ginger juice's temperature was immediately measured using a digital thermometer (Mextech ST-9283B, resolution 0.1 °C), before being collected in sterile bottles. For further qualitative analysis, samples were kept at 4 °C.

2.4 Total soluble solids, pH and temperature

The total soluble solids and pH values of the ginger juice samples were calculated using a pre-calibrated digital refractometer (RX-70001, ATAGO, Japan) and pH meter (HANNA instruments, Italy). To determine the impact of microfluidization parameters on the temperature of ginger juice, readings were taken before and after each cycle of microfluidization using a handheld thermometer.

2.5 Color

The color characteristics (L^*, a^* and b^*) of the ginger juice samples were studied using a handheld digital Chroma meter (CR- 400, Konica Minolta, Japan) calibrated using black and white reference plates as described by Koley et al., (2014). Total color difference (ΔE^*) of microfluidized ginger juice compared to control was calculated using eq. (1). Subscripts *c* and *m* represent the color values for control and microfluidized samples, respectively.

$$\Delta E^* = \sqrt{(L_c^* - L_m^*)^2 + (a_c^* - a_m^*)^2 + (b_c^* - b_m^*)^2} \quad (1)$$

2.6 Particle size analysis

The particle size distribution of ginger juice samples was analyzed using liquid-mode in PSA 1090 (Anton Paar, Austria). Debubbling and ultrasound were allowed as dispersion parameters, water was used as the solvent with a refractive index of 1.329-1.330. After cleaning the machine with deionized water, the samples were placed in the

small volume dispersion unit and uniformly dispersed with a stirrer. Measurement started when the obscuration of the samples reached about 1.5%. Measurements were taken in triplicate for each sample. Particle size measurements of all the samples were taken and analyzed by the Kalliope™ software. The results were presented in terms of D_{10}, D_{50}, and D_{90} percentile values, which represent the particle sizes below which 10%, 50%, and 90% of all particles are respectively located.

2.7 Microscopic analysis

A fluorescent microscope (Eclipse Ci-L, Nikon, Japan) was used to capture microscopic images to observe the effect of microfluidization on the extent of particle breakdown in ginger juice. Analysis was carried out by pouring 20 µL of the ginger juice samples on a clean glass slide and gently rotating the coverslip to a 45° angle to have samples with the same orientation. Images were captured using 100x magnification and white light.

2.8 Total phenolic content

The total phenolic content of the ginger juice samples was evaluated using the Folin-Ciocalteu reagent as described by Singleton et al., (1999) with some changes. In brief, diluted ginger juice samples (1:10) were mixed with 250 µL Folin-Ciocalteu reagent. Next, the mixture was added with 500 µL (7.5% sodium carbonate), and 4 ml of distilled water and incubated in the dark at 25 ºC for 2 h. After incubation, absorbance readings were taken at 725 nm using a spectrophotometer (SL159, Elico connecting science & Lab, India). Gallic acid was used (0–100 mg/mL) as a standard. Average values of three independent replications were reported in milligrams of gallic acid equivalent per 100 milliliters mg GAE/100 mL..

2.9 Antioxidant assays

2.9.1 DPPH assay

The method proposed by Mishra et al., (2011) was used to determine the antioxidant activity using the DPPH radical, with minor modifications. In brief, 3.9 mg of DPPH was dissolved in 100 mL methanol to prepare the stock solution. Then, 3.9 mL of DPPH stock solution was added to dilute ginger juice (1:20) (100 µL) followed by incubation in the dark at 25 ºC for 1 h. Also, 3.9 mL of DPPH stock solution was mixed with 100 µL methanol to prepare the control sample. Absorbance readings were taken at 517 nm using a spectrophotometer (SL159, Elico connecting science & Lab, India) and the % inhibition of DPPH was determined using equation 2.

$$\% \text{ inhibition of DPPH} = \frac{Abs\ Control - Abs\ Sample}{Abs\ Control} x\ 100 \quad (2)$$

2.9.2 ABTS assay

A mixture of ABTS stock solution (7 mM) and potassium persulfate (2.45 mM) in 1:1 v/v was kept at 25 °C for 18 h to prepare the radical cation. Then, the mixture was diluted using ethanol until it had an optical density of 0.700 at 734 nm as described by Shalaby, (2013) with minor modifications. For analysis, 1mL of stable ABTS solution was mixed with 100 µL of dilute ginger juice (1:20). Absorbance readings were taken at 734 nm using a spectrophotometer (SL159, Elico connecting science & Lab, India) after a 30 min incubation period. An ABTS solution without antioxidants was applied as the control and the % inhibition of ABTS was determined using equation 3.

$$\% \text{ inhibition of ABTS} = \frac{Abs\ Control - Abs\ Sample}{Abs\ Control} x\ 100 \quad (3)$$

2.10 Polyphenol oxidase activity

To determine the relative activity of the PPO enzyme, 500 µL of ginger juice was mixed with 2 mL of phosphate buffer (50mM, pH 6.5) followed by the addition of 1000 µL of catechol (0.2 M) as described by Tarafdar, Kaur, et al., (2021). Absorbance values were recorded at 420 nm for 0 min and at 4 min using a spectrophotometer (SL159, Elico connecting science & Lab, India). The percentage reduction in PPO activity was determined using equation 4..

$$\% \ PPO\ activity\ reduction = \left(\frac{PPO_c - PPO_m}{PPO_c}\right) \times 100 \quad (4)$$

Where, PPO_c and PPO_m are the activity of PPO in control and microfluidized ginger juice, respectively.

2.11 Microbial analysis

The total plate count was made by pouring plate count agar over 1000 µL of serially diluted (in peptone water) ginger juice sample. Similarly, yeast and molds count was carried out by pouring potato dextrose agar on 1000 µL of diluted juice sample. For total plate count and yeast and mold count, the plates were incubated for 24 h at 37 °C and 72 h at 25 °C, respectively. The results were presented in $\log_{10}$ colony forming units (CFU) per mL (Batra et al. 2016).

2.12 Statistical analysis

All the analyses were made using three independent microfluidized and control ginger juice samples. Results were

reported as averages ± standard deviations. Principal component analysis (PCA), correlation and two-way ANOVA followed by Tukey's post hoc analysis ($p<0.05$) were applied to determine the effects of microfluidization parameters (pressure and number of cycles), using OriginPro 2021, version 9.8.0.200, OriginLab Corporation, USA.

3 Results and discussion

3.1 Yield of ginger juice

After sorting, grading, cleaning and peeling the procured sample, 2.76 kg of ginger was obtained, which was further used for juice extraction. From this 2.76 kg of ginger, 1.20 L of juice was extracted. The yield of juice extraction was estimated to be 42.57% based on the juice with a density of 0.9792 g/ml, obtained from the pulp (data not shown). Because ginger contains a high percentage of non-soluble starch, nearly 50%, the juice yield was low.

3.2 TSS, pH and temperature of ginger juice

The effects of high-pressure microfluidization treatment on TSS and pH of ginger juice are summarized in Table 1. Microfluidization parameters, both pressure and number of cycles showed a significant effect ($p<0.05$) on the TSS of ginger juice. TSS decreased from 3.35% (control) to 2.70% - 3.29% after microfluidization treatment. After first microfluidization cycle, the TSS was reduced by 6.27%,19.40%, and 16.12% at 68.94, 103.42, and 137.89 MPa, respectively. Ginger juice that was subjected to a 103.42 MPa and 1-cycle treatment demonstrated the maximum TSS decrease. It should be highlighted that the first microfluidization cycle decreased the TSS, however, the second and third treatment cycles increased the TSS, with no significant difference within these cycles. This suggests that the second microfluidization cycle was effective for mass transfer from the juice particles and further solubilization in the surrounding medium. In terms of microfluidization pressure, the pressure of 103.42 MPa had a decreasing effect, whereas raising the pressure to 137.89 MPa had an increasing effect, demonstrating that a moderate microfluidization pressure has a noticeable effect on the TSS of ginger juice. TSS in the juice may be reduced due to the release of insoluble solid particles, denaturation of enzymes amylase, proteases and polygalacturonases), or the loss of the components (sugars and organic acids) that make up the soluble solids in the juice during processing (M. Chen et al. 2017). For instance, when juice is homogenized at high pressure, a little proportion of soluble protein's hydrophobic structure is revealed. Subsequently, more hydrophobic areas are produced, which reduces the protein's solubility and lowers the TSS (Guo et al. 2016). Similar results were reported after microfluidization of sugarcane (Tarafdar and Kaur 2021), sea buckthorn (Abliz et al. 2021), and pomegranate juice (M. Chen et al. 2017).

Microfluidization pressure had a significant ($p<0.05$) effect on the pH of ginger juice, whereas microfluidization

cycles had a non-significant ($p>0.05$) effect. At lower pressure (68.94 MPa), the pH value was practically identical to that of the control (6.55) (Table 1). Microfluidization pressure of 103.42 MPa caused a small increase in pH, and increasing the pressure to 137.89 MPa led to no significant difference ($p>0.05$) within these pressures. The pH value indicates the concentration of free H^+ ions. During microfluidization treatment, the breakdown of cellular components such as pectin (J. Chen et al. 2012) or proteins might reduce the concentration of free H^+, resulting in a slight increase in pH (Abliz et al. 2021).

The microfluidization treatment raised the temperature of ginger juice. The temperature of ginger juice changed the most after the first cycle and little after the second and third cycles at all microfluidization pressures (Figure 1). Overall, the maximum temperature change of 11.7 °C was recorded after the first cycle at 137.89 MPa, this increase was lower than the rise of 18 °C observed during the high pressure processing of cloudy ginger juice at 500 MPa for 10 min (D. Chen et al. 2016). Furthermore, all of the microfluidization pressures had similar final temperatures after the third cycle, and all of the final temperatures were lower than 40 °C. The temperature of the microfluidized ginger juice was raised as a result of high velocity, extreme shear, and cavitations in the interaction chamber of the microfluidizer (Dhiman and Prabhakar 2021). When the juice passes through the interaction chamber, the provided compression energy is turned into kinetic energy of the juice, which is then converted into friction energy, resulting in a temperature rise that increases as the number of cycles increase (Diels and Michiels 2006).

Table 1: TSS and pH of control and microfluidized ginger juice samples.

Microfluidization pressure (MPa)	Cycles	TSS (%)	pH
Control	0	3.35 ± 0.03^{Aa}	6.55 ± 0.03^{Bb}
68.94	1	3.14 ± 0.08^{Bc}	6.54 ± 0.02^{Ba}
	2	3.29 ± 0.05^{Bb}	6.56 ± 0.03^{Ba}
	3	3.22 ± 0.06^{Bb}	6.56 ± 0.03^{Ba}
103.42	1	2.70 ± 0.08^{Dc}	6.69 ± 0.01^{Aa}
	2	2.75 ± 0.06^{Db}	6.70 ± 0.02^{Aa}
	3	2.78 ± 0.03^{Db}	6.77 ± 0.02^{Aa}
137.89	1	2.81 ± 0.03^{Cc}	6.76 ± 0.01^{Aa}
	2	2.97 ± 0.04^{Cb}	6.70 ± 0.01^{Aa}
	3	2.94 ± 0.04^{Cb}	6.72 ± 0.02^{Aa}

Data were expressed as averages ± standard deviations from measurements of triplicate experiments. Average ± standard deviation that do not share the superscript letters capital case (pressure) and small case (cycle) are significantly different ($p < 0.05$).

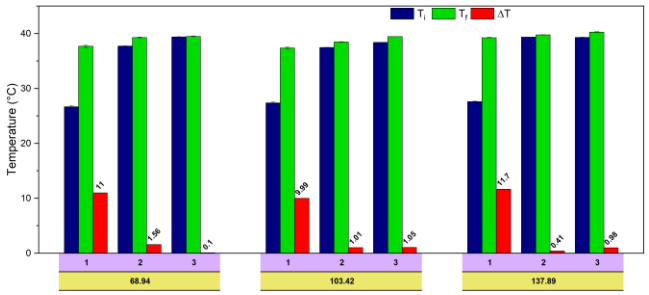

Figure 1: Change in the temperature of ginger juice after microfluidization treatment. T_i = Inlet temperature of ginger juice before microfluidization treatment (°C); T_f = Outlet temperature of ginger juice after microfluidization treatment (°C); ΔT = Rise in temperature of ginger juice due to microfluidization treatment (°C); 1, 2 and 3 on x-axis represent the number of cycles and 68.94, 103.42 and 137.89 represent the microfluidization pressure in MPa.

3.3 Color

Due to its inherent ability to predict changes in food products, color is regarded as one of the most crucial food product characteristics. Juice pigments, which are influenced by enzymatic activity, phenolic content, particle size reduction, and temperature changes, are what cause color variations in juices. The lightness of microfluidized ginger juice was significantly influenced by microfluidization pressure ($p<0.05$), but not by the number of cycles ($p<0.05$) (Table 2). At the highest pressure of 137.89 MPa, a maximum mean value of 52.85 for lightness was noted. Microfluidization increased the greenness value from -2.63 (control) to -4.06 (103.42 MPa and 1 cycle), but the effect of varying the microfluidization pressure and number of cycles was non-significant ($p>0.05$). Furthermore, microfluidized ginger juice had lower yellowness values than the control. Microfluidization pressure of 68.94 MPa reduced yellowness values from 20.97 (control) to 16.53 (3 cycles), while increasing the pressure to 103.42 MPa resulted in a non-significant ($p>0.05$) reduction, but applying pressure of 137.89 MPa resulted in a significant ($p<0.05$) reduction with a mean value of 16.88. Similarly, the number of cycles reduced the yellowness with a statistically significant ($p<0.05$) effect (Table 2). The change in color (ΔE^*) of microfluidized samples was also affected in similar pattern. Microfluidization pressures of 68.94 and 103.42 MPa had a non-significant effect ($p>0.05$) on ΔE^*, while a pressure of 137.89 MPa caused a significant ($p<0.05$) increase. Additionally, the number of cycles had a significant ($p<0.05$) effect, ΔE^* increasing with the number of cycles. Thereby, a maximum ΔE^* of 5.18 was observed at 137.89 MPa and 3 cycles. Karacam et al., (2015) observed similar patterns after the microfluidization of strawberry juice. Also, hydrodynamic cavitation processing showed reduction in yellowness of aonla juice with an increase in pressure (Annapoorna et al. 2023). Curcumin, demethoxycurcumin, and 6-

dehydrogingerdione were identified as the major compounds responsible for ginger's yellow color (Yamaguchi et al. 2010). Color is influenced not only by the pigment content of the food, but also by its physical structure and light-scattering capabilities. Microfluidization reduces particle size (Table 3), which increases surface area and, as a result, light-scattering properties (Sharma et al. 2021).

Table 2: Color parameters of control and microfluidized ginger juice.

Microfluidization pressure (MPa)	Cycles	L^*	a^*	b^*	ΔE
Control	0	52.08 ± 0.88^{Bb}	-2.63 ± 0.55^{Aa}	20.97 ± 0.57^{Aa}	-
68.94	1	52.84 ± 0.39^{ABa}	-3.60 ± 0.31^{Bb}	18.54 ± 0.37^{Bb}	2.76 ± 0.39^{Bc}
	2	52.37 ± 0.29^{ABab}	-3.75 ± 0.15^{Bb}	17.25 ± 0.48^{Bc}	3.90 ± 0.46^{Bb}
	3	52.68 ± 0.47^{ABab}	-4.01 ± 0.61^{Bb}	16.53 ± 0.16^{Bd}	4.73 ± 0.18^{Ba}
103.42	1	52.54 ± 0.10^{Ba}	-4.06 ± 0.12^{Bb}	17.92 ± 0.17^{BCb}	3.41 ± 0.15^{Bc}
	2	52.24 ± 0.11^{Bab}	-3.77 ± 0.10^{Bb}	17.25 ± 0.26^{BCc}	3.90 ± 0.25^{Bb}
	3	52.47 ± 0.27^{Bab}	-3.93 ± 0.10^{Bb}	16.73 ± 0.10^{BCd}	4.46 ± 0.03^{Ba}
137.89	1	52.85 ± 0.14^{Aa}	-3.62 ± 0.11^{Bb}	17.67 ± 0.10^{Cb}	3.54 ± 0.10^{Ac}
	2	53.13 ± 0.19^{Aab}	-3.94 ± 0.10^{Bb}	17.10 ± 0.13^{Cc}	4.27 ± 0.18^{Ab}
	3	52.76 ± 0.10^{Aab}	-3.63 ± 0.10^{Bb}	15.94 ± 0.10^{Cd}	5.18 ± 0.10^{Aa}

Data were expressed as averages ± standard deviations from measurements of triplicate experiments. Average ± standard deviation that do not share the superscript letters capital case (pressure) and small case (cycle) are significantly different ($p < 0.05$).

Table 3: Particle size of control and microfluidized ginger juice.

Microfluidization pressure (MPa)	Cycles	D_{10} (µm)	D_{50} (µm)	D_{90} (µm)	Mean particle size (µm)
Control	0	4.02 ± 0.01^{Aa}	16.04 ± 0.02^{Aa}	24.03 ± 0.63^{Aa}	15.85 ± 0.07^{Aa}
68.94	1	3.60 ± 0.05^{Ab}	14.34 ± 0.11^{BCb}	23.06 ± 0.52^{ABab}	14.56 ± 0.10^{Bb}
	2	3.92 ± 0.05^{Aa}	14.51 ± 0.10^{BCb}	21.66 ± 1.06^{Abb}	14.57 ± 0.09^{Bb}
	3	4.25 ± 0.33^{Aab}	14.63 ± 0.13^{BCb}	22.14 ± 1.41^{ABab}	14.83 ± 0.05^{Bb}
103.42	1	4.04 ± 0.01^{Ab}	15.50 ± 0.16^{Bb}	23.35 ± 1.07^{ABab}	14.72 ± 0.14^{Bb}
	2	4.05 ± 0.02^{Aa}	14.57 ± 0.19^{Bb}	22.62 ± 0.54^{Abb}	14.68 ± 0.20^{Bb}

	3	3.61 ± 0.09^{Aab}	14.10 ± 0.10^{Bb}	22.57 ± 0.60^{ABab}	14.06 ± 0.10^{Bb}
137.89	1	2.63 ± 0.04^{Bb}	13.25 ± 0.10^{Cb}	21.89 ± 1.08^{Bab}	12.86 ± 0.11^{Cb}
	2	3.55 ± 0.07^{Ba}	14.35 ± 0.22^{Cb}	22.46 ± 0.94^{Bb}	13.16 ± 0.10^{Cb}
	3	3.54 ± 0.11^{Bab}	14.39 ± 0.15^{Cb}	22.32 ± 1.05^{Bab}	13.19 ± 0.07^{Cb}

Data were expressed as averages ± standard deviations from measurements of triplicate experiments. Average ± standard deviation that do not share the superscript letters capital case (pressure) and small case (cycle) are significantly different ($p < 0.05$).

3.4 Particle size

Particle size plays a significant role in the rheological and sedimentation properties of juice, as well as in its appearance and changes at the macromolecular level. When compared to the control sample, the microfluidization treatment decreased the D_{10}, D_{50}, D_{90}, and mean particle size of ginger juice. Microfluidization pressure significantly ($p<0.05$) decreased the D_{10} particle size from 4.02 µm (control) to 2.63 µm (137.89 MPa and 1 cycle), whereas the number of cycles caused D_{10} particle size to increase significantly ($p<0.05$) up to the second microfluidization cycle treatment. Further increase in the number of cycles had a statistically non-significant ($p>0.05$) effect, but the values were still lower than the control sample (Table 3). Surprisingly, the D_{10} particle size was found to be 4.25 µm at a microfluidization pressure of 62.94 MPa and 3 cycles, which is higher than that of the control sample. With an increase in microfluidization pressure, the D_{50} particle size showed a statistically significant ($p<0.05$) reduction of about 2 µm and a statistically non-significant ($p>0.05$) increase with an increase in the number of cycles, but it did not exceed the value of the control sample (16.034 µm). In addition, the microfluidization treatment lead to a reduction in the D_{90} particle size of ginger juice compared to the control sample. However, altering the microfluidization parameters, including both pressure and number of cycles, did not show any statistically significant ($p>0.05$) effect on the D_{90} particle size. Comparing the treated samples to the control sample, microfluidization decreased the mean particle size. When the microfluidization pressure was increased, the mean particle size decreased significantly ($p<0.05$), with mean values of 14.65, 14.48, and 13.07 µm at 68.94, 103.42, and 137.89 MPa, respectively. When the number of cycles were increased, the mean particle size increased, but the effect was not statistically significant ($p>0.05$). Overall, a common pattern observed was a decrease in the particle size with an increase in pressure, and an increase in the particle size with an increase in the number of cycles at the same pressure. Similar results were observed with the microfluidization of sea buckthorn juice by Abliz et al., (2021) at different pressure-cycles combinations. Aggregation of protein particles at high temperatures justified the increase in particle size with an increase in the number of cycles, which may be similar to ginger juice as the

temperature of microfluidized ginger juice increases with an increase in the number of cycles (Figure 1). Moreover, microfluidization works on the combination of powerful shear, high frequency vibration, high velocity impact, instantaneous pressure drops and cavity effect (Suhag et al. 2021). The multiple forces produced in microfluidization could lead to a smaller particle size of ginger juice with an increase in the microfluidization pressure. Similar, observations of reduction in particle with increase in pressure were made by Annapoorna et al. (2023) for hydrodynamic cavitation processed aonla juice due to shockwaves, strong turbulence, and violent collapsing of microbubbles to form microjets. Furthermore, changes in particle size may be due to changes in starch, as increasing pressure changes the structure, crystallinity, gelatinization temperature, enthalpy of gelatinization, and solubility of starch (X. M. Wang et al. 2018). Microscopic analysis (discussed in section 3.5) revealed that the small starch particles tend to aggregate into larger ones. This aggregation process may result from partial gelatinization (Song et al. 2013), and it could be the underlying cause for the observed changes in particle size of microfluidized ginger juice. .

3.5 Microscopic analysis

The control sample showed higher aggregation than all other samples, which broke down more as the pressure increased. A decrease in particle size with an increase in pressure can be observed in Figure 2. Among the three pressure levels, the maximum decrease in particle size can be observed at 137.89 MPa, compared to 68.94 and 103.42 MPa. These findings imply that following microfluidization treatment, more cellular contents are liberated. At the same time, more tiny particles made of bits of cell wall and cell contents started to appear. The findings of Jurić et al., (2019) also demonstrated that after homogenization, cell clusters and cell walls were damaged. Particle disruption may cause intact cell walls to rupture, disrupted cells to break, and disrupted cells to release intracellular components, changing the composition, size, and polydispersity of suspended particles (Rojas et al. 2016). However, an increase in the number of cycles showed an increase in the mean diameter at the same pressure, which might be due to the formation of aggregates. Overall, the microscope images showed a gradual disruption of ginger juice cells with increasing microfluidization pressure, which aligns with the reduction in particle size displayed in Table 3.

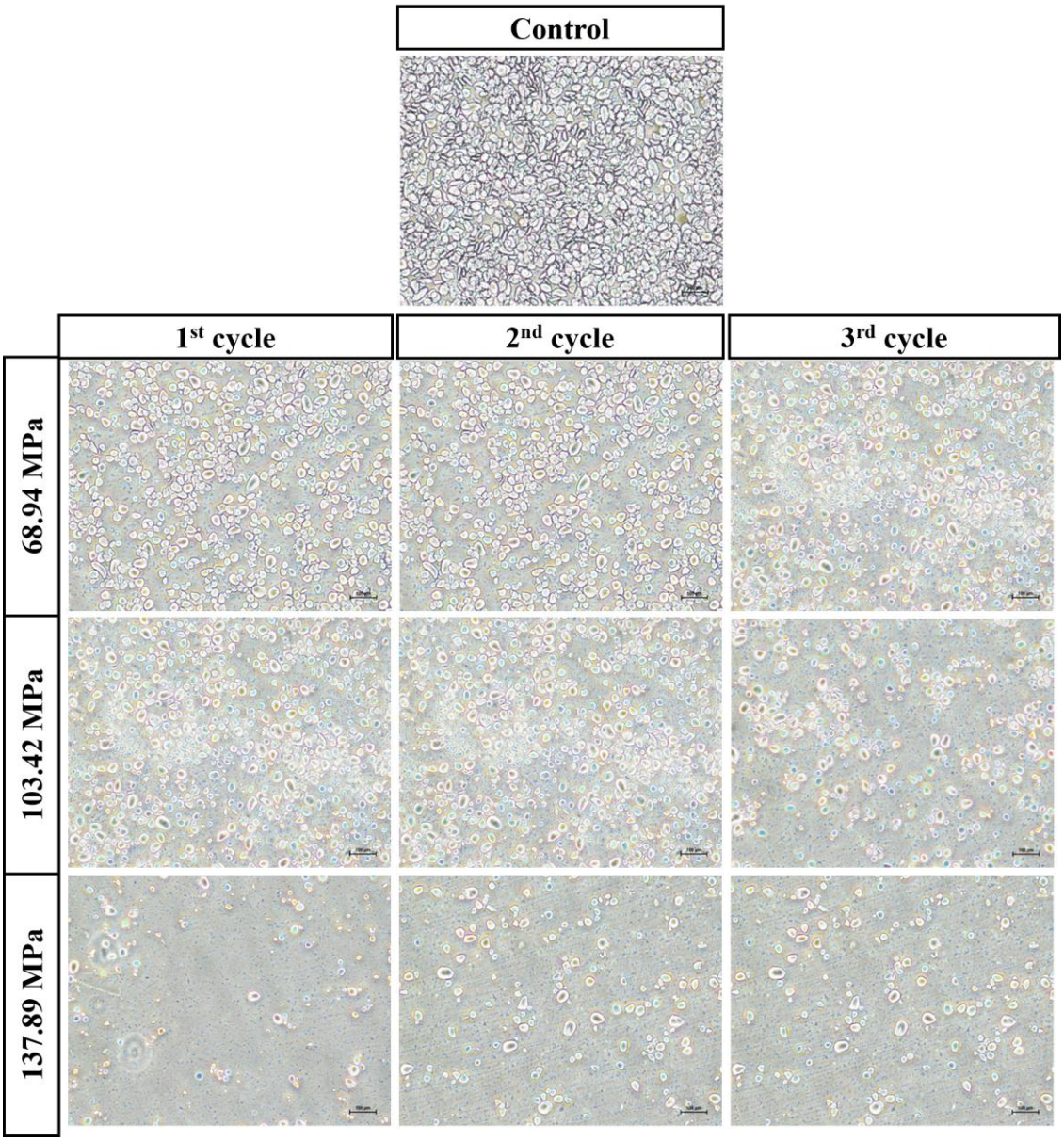

Figure 2: Control and microfluidized ginger juice under 100x microscope view – the providence of particles.

3.6 Total phenolic content

The total phenolic content of the ginger juice samples shown in Table 4 was analyzed using the Folin-Ciocalteu method. Total phenolic content was significantly ($p<0.05$) affected by microfluidization cycles, whereas pressure had a non-significant ($p>0.05$) effect. The total phenolic content of the control sample was 56.79 mg GAE/100 mL, which was close to the value of 57.40 mg GAE/100 mL for cloudy ginger juice reported by Chen et al., (2016). In comparison to the control, the total phenolic content decreased considerably after the first microfluidization cycle at

68.94 MPa, with a mean value of 51.35 mg GAE/100 mL. This decrease after first microfluidization cycle can be attributed to the loss of heat-sensitive ginger's sesquiterpene compounds, which form phenolic compounds (Jugreet et al. 2020), due to localized heat generation ($\Delta T = 11°C$) inside the interaction chamber. However, the total phenolic content increased to a mean value of 63.36 (68.94 MPa, second cycle) and 65.28 mg GAE/100 mL (103.42 MPa, third cycle), both of which were higher than the control value. This increase in the total phenolic content can only be explained by considering that the disruption of cellular membrane and release of intracellular material, phenolic compounds and pigments dominated the thermal breakdown brought about by the small increase in the temperature ($\Delta T = 1.56°C$ and $1.05°C$). Similarly, the increased total phenolic content of ginger after convective drying at 60°C was attributed to the release of bound phenolic compounds brought about by the breakdown of cell wall (Mustafa and Chin 2023). Comparable results were described by Tarafdar, Kumar, et al., (2021), showing a significant effect of the number of cycles and no prominent impact of microfluidization pressure on the total phenolic content of sugarcane juice.

Table 4: Total phenolic content and antioxidant activity of control and microfluidized ginger juice.

Microfluidization pressure (MPa)	Cycles	Total phenolic content (mg GAE/ 100 mL)	DPPH (% inhibition)	ABTS (% inhibition)
Control	0	56.79 ± 0.26^{Aab}	69.99 ± 0.10^{Aab}	74.61 ± 0.16^{Aab}
68.94	1	51.35 ± 0.30^{Ab}	56.63 ± 0.10^{Ab}	73.20 ± 0.16^{Ab}
	2	63.36 ± 0.20^{Aab}	72.49 ± 0.17^{Aa}	82.13 ± 0.20^{Aab}
	3	53.44 ± 0.19^{Aa}	67.50 ± 0.21^{Aa}	73.67 ± 0.12^{Aa}
103.42	1	47.23 ± 0.29^{Ab}	59.24 ± 0.11^{Ab}	70.85 ± 0.10^{Ab}
	2	52.13 ± 0.10^{Aab}	63.34 ± 0.26^{Aa}	74.61 ± 0.14^{Aab}
	3	65.28 ± 0.14^{Aa}	77.51 ± 0.22^{Aa}	84.74 ± 0.18^{Aa}
137.89	1	56.50 ± 0.28^{Ab}	69.75 ± 0.10^{Ab}	79.99 ± 0.24^{Ab}
	2	56.21 ± 0.12^{Aab}	69.64 ± 0.15^{Aa}	80.09 ± 0.16^{Aab}
	3	58.05 ± 0.13^{Aa}	69.50 ± 0.40^{Aa}	81.40 ± 0.10^{Aa}

Data were expressed as averages ± standard deviations from measurements of triplicate experiments. Average ± standard deviation that do not share the superscript letters capital case (pressure) and small case (cycle) are significantly different ($p < 0.05$).

3.7 Antioxidant activity

To assess the antioxidant activity of ginger juice, DPPH and ABTS radicals were utilized as stable free radicals (Öztürk et al. 2007). Because of their potential to donate hydrogen atoms or electrons and trap free radicals, plant

extracts containing polyphenolic components exhibit antioxidant scavenging activity. DPPH scavenging activity showed no significant ($p>0.05$) trend with an increase in pressure, and also no noticeable increase was observed with respect to the control, except at 103.42 MPa and 3 cycles, which was 7.513 % more than that of control (Table 4). DPPH scavenging activity and total phenolic content showed a strong correlation ($R^2 = 0.91$), which helps to explain that maybe total phenolic compounds are the cause of the irregular trend. Similarly, for the ABTS assay, the influence of the microfluidization treatment was irregular. In our study, the irregular effect of microfluidization on antioxidant activity appears to be an inconsistent result. One interesting phenomenon was that the maximum values for total phenolic content, DPPH scavenging, and ABTS antioxidant activity were all found at 103.42 MPa and the third cycle. This variation in the findings of different assays may be explained by the fact that these assays are influenced by various parameters such as the technique used, free radical generators used, and the complexity of the molecular structure being tested (X. Wang et al. 2019). Similar findings and inferences on the DPPH and ABTS assay for microfluidized peach juice were published by Wang et al., (2019).

3.8 Enzymatic activity

Polyphenol oxidase (PPO) activity was investigated to determine the change in enzymatic activity following microfluidization treatment (Table 5). The microfluidization parameters, both pressure and number of cycles, caused no significant ($p>0.05$) reduction in the PPO activity of ginger juice. Although a decrease of about 2% compared to the control was observed, this change is not significant enough to warrant using this technology to reduce the enzymatic activity of ginger juice. The activity of PPO in various fruit and vegetable juices has been shown to be affected differently by microfluidization treatment. In sugarcane juice, PPO activity decreased significantly ($p<0.05$) after microfluidization, according to Tarafdar, Kaur, et al., (2021). They also reported that sugarcane stems were blanched before the extraction of juice, which may facilitate microfluidization to reduce the enzymatic activity. While, Liu et al., (2009) found a considerable rise in the relative PPO activity in Chinese pear. They reported an increase of 85.01% after microfluidization at 160 MPa and 3 cycles. Additionally, a reduction in enzymatic activity is associated with changes in tertiary and quaternary structures brought on by the dissolution of a non-covalent hydrogen bond, which typically requires pressures greater than 150 MPa (Porto et al. 2018). However, the maximum pressure used in our study was 137.89 MPa, which could explain the insignificant reduction in ginger juice enzymatic activity. Furthermore, Leite Júnior et al., (2016) predicted that it would be challenging to anticipate the impact of high pressures on the inactivation of enzymes due to the involvement of multifactorial parameters, such as

operational parameters, sample pretreatments, product features, and enzyme characteristics.

Table 5: Polyphenol oxidase (PPO) enzyme activity and microbial count for control and microfluidized ginger juice.

Microfluidization pressure (MPa)	Cycles	% PPO activity reduction	Total plate count (log_{10} CFU/mL)	Yeast and mold count (log_{10} CFU/mL)
Control	0	-	6.63 ± 0.02^{Aa}	6.55 ± 0.02^{Aa}
68.94	1	1.83 ± 0.01^{Aa}	6.57 ± 0.02^{Bb}	6.53 ± 0.02^{Ab}
	2	1.14 ± 0.02^{Aa}	6.51 ± 0.01^{Bbc}	6.48 ± 0.02^{Ab}
	3	1.68 ± 0.03^{Aa}	6.47 ± 0.03^{Bc}	6.36 ± 0.01^{Ac}
103.42	1	1.93 ± 0.03^{Aa}	6.01 ± 0.02^{Cb}	5.21 ± 0.04^{Bb}
	2	1.56 ± 0.05^{Aa}	6.00 ± 0.05^{Cbc}	5.04 ± 0.04^{Bb}
	3	1.48 ± 0.01^{Aa}	5.97 ± 0.03^{Cc}	4.79 ± 0.11^{Bc}
137.89	1	1.17 ± 0.02^{Aa}	ND	ND
	2	2.34 ± 0.02^{Aa}	ND	ND
	3	1.95 ± 0.02^{Aa}	ND	ND

ND: Not detected; Data were expressed as averages ± standard deviations from measurements of triplicate experiments. Average ± standard deviation that do not share the superscript letters capital case (pressure) and small case (cycle) are significantly different ($p < 0.05$).

3.9 Microbiological analysis

The microbial count of control and microfluidized ginger juice is displayed in Table 5. The total plate, yeast, and mold counts in ginger juice were significantly ($p<0.05$) influenced by microfluidization parameters. As the microfluidization pressure and number of cycles increased, the total plate, yeast, and mold count decreased. The microbes in ginger juice could not be completely destroyed by lower pressures of 68.94 and 103.42 MPa and 3 cycles. In contrast, the pressure of 137.89 MPa and 1 cycle was able to completely reduce the microbial count, producing a ginger juice that was microbiologically safe in terms of both aerobic and yeast and mold count, indicating that this pressure was safe and effective. Microfluidization exerts its main mechanism of destroying vegetative bacteria through mechanical forces, which encompass spatial pressure, turbulence, impingement, cavitations, and/or velocity gradients within the liquid(Diels and Michiels 2006). According to Aertsen et al., (2009), the increased pressure causes changes in membrane fluidity, protein denaturation, and RNA transcription, all of which contribute to the inactivation of microorganisms. Diels & Michiels, (2006) asserted that the random motion of numerous eddies of different sizes is what causes velocity changes upon microfluidization. Eddies smaller than the cell dimensions produce an oscillating action of cell and cell fluid due to forces varying in intensity and scale, ultimately disrupting the cell. While, eddies larger than the cell dimensions cause the cell to be displaced.

Furthermore, it is known that high pressure cycling is more effective than continuous high pressure processing for killing vegetative microbes (Maresca et al. 2011).

3.10 Principal component analysis (PCA)

Biplot of principle component analysis shown in Figure 3 explained nearly 68% of total variance. Data was widely scattered for the different pressure and cycles combinations, suggesting that these combinations significantly influenced the physico-chemical and functional attributes of ginger juice. Furthermore, as the number of cycles increased, the score points for the lower (68.94 MPa) and moderate (103.42 MPa) microfluidization pressures became increasingly scattered, signifying that the number of cycles had a greater impact at these pressure levels. Conversely, the score points for the higher (137.89 MPa) microfluidization pressure remained more consistent as the number of cycles increased, implying that the number of cycles had less of an effect at this pressure level. Loadings of antioxidant assays (DPPH and ABTS) and total phenolic content were in the same direction, indicating a positive correlation, as expected, given that the phenols contained in ginger juice may contribute to its antioxidant activity (Tanweer et al. 2020). Furthermore, the antioxidant assays and total phenolic content loadings clustered near ginger juice microfluidized at 103.42 MPa and 3 cycles, showing that this pressure cycle combination is suitable for delivering ginger juice rich in phenolic compounds and enhanced antioxidant activity. Although the loadings of PPO exhibited no cluster close to any pressure-cycle combination, indicating that the processing conditions used in this study failed to inactivate the PPO enzyme present in the ginger juice.

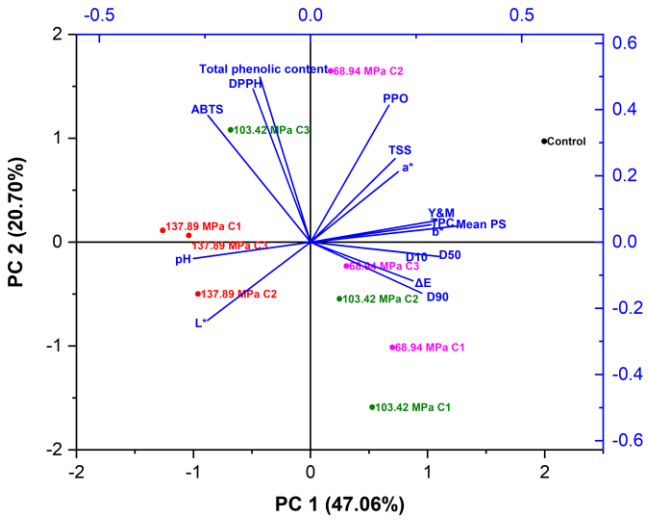

Figure 3: Principal component analysis (PCA) score and loading plot of PC1 and PC2 of ginger rhizome juice. Where, TSS – total soluble solids, L*- lightness, a*- redness, b*- yellowness, ΔE - total color difference, D10, D50, D90 - the particle sizes below which 10%, 50%, and 90% of all particles are respectively located, Mean PS – mean particle size, DPPH - % inhibition of DPPH, ABTS - % inhibition of ABTS, PPO - % Polyphenol oxidase activity reduction, TPC – total plate count, Y&M – yeast and mold count, C1, C2 and C3 – number of cycles.

4 Conclusion

Microfluidization significantly affected the physico-chemical properties of ginger rhizome juice with minimal effect on the polyphenol oxidase enzyme. Ginger rhizome juice underwent mild heating during microfluidization, with a final temperature of less than 40°C. In addition, the microfluidization process resulted in a reduction in particle size by cell breakage, which releases phenolic components and pigments, in turn affecting the antioxidant and color characteristics. A higher microfluidization pressure of 137.89 MPa was effective in completely reducing the aerobic microbes as well as the yeasts and molds, resulting in a microbes free ginger juice with increased antioxidant activity. Overall, the microfluidization technique has the potential to deliver clean-label, safe, and high-quality ginger juice. Also, microfluidized ginger rhizome juice may be used for the production of stable flavored beverages such as ginger ale, ginger beer, ginger-infused teas, smoothies, as well as functional foods like energy bars, health shots, and nutritional supplements. Further research will focus on the changes in volatile components, sensory aspects, storage quality analysis and the development of different juice blends of ginger juice using microfluidization treatment and the commercialization of microfluidized juices.

Acknowledgement

The infrastructural support received from the National Institute of Food Technology Entrepreneurships and Management, Sonipat-131028, Haryana, India is greatly acknowledged. Authors would like to thank Mr. Mutasem Razem (Faculty of Science and Technology, Free University of Bozen-Bolzano, Italy) for his valuable inputs to improve the overall quality of manuscript.

Funding

No funding was received to conduct this study.

Authors' contributions

Rajat Suhag: Conceptualization, Methodology, Formal analysis, Investigation, Data curation, Writing – original draft, Writing-revision and editing. **Shivam Singh:** Formal analysis, Investigation, Data curation. **Yogesh Kumar**: Formal analysis, Investigation, Data curation, Writing – original draft. **Pramod K Prabhakar:** Conceptualization, Writing-revision and editing, Project administration, Supervision. **Murlidhar Meghwal:** Conceptualization, Writing-revision and editing, Project administration, Supervision.

All authors read and approved the final manuscript.

Competing interests

The authors have no relevant financial or non-financial interests to disclose.

Availability of data and material/ Data availability

Data available on request to the corresponding author.

References

Abliz, A., Liu, J., Mao, L., Yuan, F., & Gao, Y. (2021). Effect of dynamic high pressure microfluidization treatment on physical stability, microstructure and carotenoids release of sea buckthorn juice. *LWT*. https://doi.org/10.1016/j.lwt.2020.110277

Aertsen, A., Meersman, F., Hendrickx, M. E. G., Vogel, R. F., & Michiels, C. W. (2009). Biotechnology under high pressure: applications and implications. *Trends in Biotechnology*. https://doi.org/10.1016/j.tibtech.2009.04.001

Ali, B. H., Blunden, G., Tanira, M. O., & Nemmar, A. (2008). Some phytochemical, pharmacological and toxicological properties of ginger (Zingiber officinale Roscoe): a review of recent research. *Food and chemical Toxicology*, *46*(2), 409–420.

Annapoorna, R. P., More, P. R., & Arya, S. S. (2023). Effect of pressure and time on bioactive content, PPO inactivation, physicochemical and sensory properties of aonla (Emblica officinalis) juice during hydrodynamic cavitation processing. *Food Science and Biotechnology*, *32*(1), 71–82. https://doi.org/10.1007/s10068-022-01164-2

Artiga-Artigas, M., Molet-Rodríguez, A., Salvia-Trujillo, L., & Martín-Belloso, O. (2019). Formation of Double (W1/O/W2) Emulsions as Carriers of Hydrophilic and Lipophilic Active Compounds. *Food and Bioprocess*

Technology, *12*(3), 422–435. https://doi.org/10.1007/s11947-018-2221-3

Ban, Z., Zhang, J., Li, L., Luo, Z., Wang, Y., Yuan, Q., et al. (2020). Ginger essential oil-based microencapsulation as an efficient delivery system for the improvement of Jujube (Ziziphus jujuba Mill.) fruit quality. *Food Chemistry*. https://doi.org/10.1016/j.foodchem.2019.125628

Bandyopadhyay, M., Chakraborty, R., & Raychaudhuri, U. (2008). Antioxidant activity of natural plant sources in dairy dessert (Sandesh) under thermal treatment. *LWT*. https://doi.org/10.1016/j.lwt.2007.06.001

Batra, N. G., Sharma, A., & Agarwal, N. (2016). Microbiological analysis of packed fruit juices locally available in Jaipur, India. *International Journal of Pharma and Bio Sciences*. https://doi.org/10.22376/ijpbs.2016.7.4.b395-401

Bitik, A., Sumnu, G., & Oztop, M. (2019). Physicochemical and Structural Characterization of Microfluidized and Sonicated Legume Starches. *Food and Bioprocess Technology*, *12*(7), 1144–1156. https://doi.org/10.1007/s11947-019-02264-4

Chakraborty, S., Rao, P. S., & Mishra, H. N. (2016). Changes in Quality Attributes During Storage of High-Pressure and Thermally Processed Pineapple Puree. *Food and Bioprocess Technology*, *9*(5), 768–791. https://doi.org/10.1007/s11947-015-1663-0

Chen, D., Pan, S., Chen, J., Pang, X., Guo, X., Gao, L., et al. (2016). Comparing the Effects of High Hydrostatic Pressure and Ultrahigh Temperature on Quality and Shelf Life of Cloudy Ginger Juice. *Food and Bioprocess Technology*. https://doi.org/10.1007/s11947-016-1759-1

Chen, F., Tang, Y., Sun, Y., Veeraraghavan, V. P., Mohan, S. K., & Cui, C. (2019). 6-shogaol, a active constiuents of ginger prevents UVB radiation mediated inflammation and oxidative stress through modulating NrF2 signaling in human epidermal keratinocytes (HaCaT cells). *Journal of Photochemistry and Photobiology B: Biology*. https://doi.org/10.1016/j.jphotobiol.2019.111518

Chen, J., Liang, R. H., Liu, W., Liu, C. M., Li, T., Tu, Z. C., & Wan, J. (2012). Degradation of high-methoxyl pectin by dynamic high pressure microfluidization and its mechanism. *Food Hydrocolloids*. https://doi.org/10.1016/j.foodhyd.2011.12.018

Chen, M., Xu, Y., & Zong, W. (2017). Effect of ultra-high pressure micro-jet on the quality of pomegranate juice. *Food Research and Development*, *38*(3), 81–85. https://doi.org/10.3969/j.issn.1005- 6521.2017.03.018.

Cui, Y., Shi, Y., Bao, Y., Wang, S., Hua, Q., & Liu, Y. (2018). Zingerone attenuates diabetic nephropathy through

518 inhibition of nicotinamide adenine dinucleotide phosphate oxidase 4. *Biomedicine and Pharmacotherapy*.
519 https://doi.org/10.1016/j.biopha.2018.01.051
520 Dammak, I., & do Amaral Sobral, P. J. (2017). Formulation and Stability Characterization of Rutin-Loaded Oil-in-
521 Water Emulsions. *Food and Bioprocess Technology*, *10*(5), 926–939. https://doi.org/10.1007/s11947-017-
522 1876-5
523 Dhiman, A., & Prabhakar, P. K. (2021). Micronization in food processing: A comprehensive review of mechanistic
524 approach, physicochemical, functional properties and self-stability of micronized food materials. *Journal of*
525 *Food Engineering*, *292*, 110248. https://doi.org/10.1016/j.jfoodeng.2020.110248
526 Diels, A. M. J., & Michiels, C. W. (2006). High-pressure homogenization as a non-thermal technique for the
527 inactivation of microorganisms. *Critical Reviews in Microbiology*.
528 https://doi.org/10.1080/10408410601023516
529 Espinosa-Solís, V., García-Tejeda, Y. V., Portilla-Rivera, O. M., & Barrera-Figueroa, V. (2021). Tailoring Olive Oil
530 Microcapsules via Microfluidization of Pickering o/w Emulsions. *Food and Bioprocess Technology*.
531 https://doi.org/10.1007/s11947-021-02673-4
532 Gabbi, D. K., Bajwa, U., & Goraya, R. K. (2018). Physicochemical, melting and sensory properties of ice cream
533 incorporating processed ginger (Z ingiber officinale). *International Journal of Dairy Technology*, *71*(1), 190–
534 197. https://doi.org/10.1111/1471-0307.12430
535 Grand View Research. (2022). *Fruit And Vegetable Juice Market Size, Share & Trends Analysis Report By Product*
536 *(Fruit, Vegetable Juices), By Distribution Channel (Supermarkets/Hypermarkets, Online), By Region, And*
537 *Segment Forecasts, 2022 - 2030*. https://www.grandviewresearch.com/industry-analysis/fruit-vegetable-juice-
538 market#:~:text=b.,USD 138.54 billion in 2022.
539 Guo, X. J., Zong, W., Zhao, G. Y., Zhang, L. H., Wang, X. Y., & Wu, S. H. (2016). Effect of high pressure
540 microfluidization (HPM) on the physical stability of yam juice. *Science and Technology of Food Industry*,
541 *37*(17), 125–128.
542 Jugreet, B. S., Suroowan, S., Rengasamy, R. R. K., & Mahomoodally, M. F. (2020). Chemistry, bioactivities, mode
543 of action and industrial applications of essential oils. *Trends in Food Science and Technology*.
544 https://doi.org/10.1016/j.tifs.2020.04.025
545 Jurić, S., Ferrari, G., Velikov, K. P., & Donsì, F. (2019). High-pressure homogenization treatment to recover

546 bioactive compounds from tomato peels. *Journal of Food Engineering*.
547 https://doi.org/10.1016/j.jfoodeng.2019.06.011
548 K Gaikwad, K. (2012). Studies on the Development and Shelf Life of Low Calorie Herbal Aonla- Ginger RTS
549 Beverage by Using Artificial Sweeteners. *Journal of Food Processing & Technology*, *04*(01).
550 https://doi.org/10.4172/2157-7110.1000200
551 Karacam, C. H., Sahin, S., & Oztop, M. H. (2015). Effect of high pressure homogenization (microfluidization) on
552 the quality of Ottoman Strawberry (F. Ananassa) juice. *LWT*. https://doi.org/10.1016/j.lwt.2015.06.064
553 Ke, Y., Chen, J., Dai, T., Xiao, M., Chen, M., Liang, R., et al. (2022). Industry-Scale Microfluidizer: a Novel
554 Technology to Improve Physiochemical Qualities and Volatile Flavor of Whole Mango Juice. *Food and*
555 *Bioprocess Technology*. https://doi.org/10.1007/s11947-022-02979-x
556 Koley, T. K., Nishad, J., Kaur, C., Su, Y., Sethi, S., Saha, S., et al. (2020a). Effect of high-pressure microfluidization
557 on nutritional quality of carrot (Daucus carota L.) juice. *Journal of Food Science and Technology*.
558 https://doi.org/10.1007/s13197-020-04251-6
559 Koley, T. K., Nishad, J., Kaur, C., Su, Y., Sethi, S., Saha, S., et al. (2020b). Effect of high-pressure
560 microfluidization on nutritional quality of carrot (Daucus carota L.) juice. *Journal of Food Science and*
561 *Technology*, *57*(6), 2159–2168. https://doi.org/10.1007/s13197-020-04251-6
562 Koley, T. K., Singh, S., Khemariya, P., Sarkar, A., Kaur, C., Chaurasia, S. N. S., & Naik, P. S. (2014). Evaluation of
563 bioactive properties of Indian carrot (Daucus carota L.): A chemometric approach. *Food Research*
564 *International*, *60*, 76–85. https://doi.org/10.1016/j.foodres.2013.12.006
565 Kumar, A., Dhiman, A., Suhag, R., Sehrawat, R., Upadhyay, A., & McClements, D. J. (2022). Comprehensive
566 review on potential applications of microfluidization in food processing. *Food Science and Biotechnology*,
567 *31*(1), 17–36. https://doi.org/10.1007/s10068-021-01010-x
568 Leite Júnior, B. R. de C., Tribst, A. A. L., & Cristianini, M. (2016). Comparative effects of high isostatic pressure
569 and thermal processing on the inactivation of Rhizomucor miehei protease. *LWT - Food Science and*
570 *Technology*. https://doi.org/10.1016/j.lwt.2015.09.042
571 Liu, W. E. I., Jianhua, L. I. U., Mingyong, X. I. E., Chengmei, L. I. U., Weilin, L. I. U., & Wan, J. I. E. (2009).
572 Characterization and high-pressure microfluidization-induced activation of polyphenoloxidase from chinese
573 pear (Pyrus pyrifolia Nakai). *Journal of Agricultural and Food Chemistry*. https://doi.org/10.1021/jf9006642

Liu, Y., Zhang, W., Wang, K., Bao, Y., Regenstein, J. Mac, & Zhou, P. (2019). Fabrication of Gel-Like Emulsions with Whey Protein Isolate Using Microfluidization: Rheological Properties and 3D Printing Performance. *Food and Bioprocess Technology*, *12*(12), 1967–1979. https://doi.org/10.1007/s11947-019-02344-5

Maresca, P., Donsì, F., & Ferrari, G. (2011). Application of a multi-pass high-pressure homogenization treatment for the pasteurization of fruit juices. *Journal of Food Engineering*. https://doi.org/10.1016/j.jfoodeng.2010.12.030

Mert, B., Tekin, A., Demirkesen, I., & Kocak, G. (2014a). Production of Microfluidized Wheat Bran Fibers and Evaluation as an Ingredient in Reduced Flour Bakery Product. *Food and Bioprocess Technology*, *7*(10), 2889–2901. https://doi.org/10.1007/s11947-014-1258-1

Mert, B., Tekin, A., Demirkesen, I., & Kocak, G. (2014b). Production of Microfluidized Wheat Bran Fibers and Evaluation as an Ingredient in Reduced Flour Bakery Product. *Food and Bioprocess Technology*, *7*(10), 2889–2901. https://doi.org/10.1007/s11947-014-1258-1

Microfluidics chamber user guide. (2015). https://www.alfatest.it/keyportal/uploads/2017-microfluidics-chamber-user-guide.pdf

Mishra, B. B., Gautam, S., & Sharma, A. (2011). Shelf Life Extension of Sugarcane Juice Using Preservatives and Gamma Radiation Processing. *Journal of Food Science*. https://doi.org/10.1111/j.1750-3841.2011.02348.x

Mustafa, I., & Chin, N. L. (2023). Antioxidant Properties of Dried Ginger (Zingiber officinale Roscoe) var. Bentong. *Foods*, *12*(1), 178. https://doi.org/10.3390/foods12010178

Oliete, B., Potin, F., Cases, E., & Saurel, R. (2019). Microfluidization as Homogenization Technique in Pea Globulin-Based Emulsions. *Food and Bioprocess Technology*. https://doi.org/10.1007/s11947-019-02265-3

Öztürk, M., Aydoğmuş-Öztürk, F., Duru, M. E., & Topçu, G. (2007). Antioxidant activity of stem and root extracts of Rhubarb (Rheum ribes): An edible medicinal plant. *Food Chemistry*, *103*(2), 623–630. https://doi.org/10.1016/j.foodchem.2006.09.005

Pinto, S. V, Patel, A. M., Jana, A. H., & Solanky, M. J. (2009). Evaluation of different forms of ginger as flavouring in herbal ice cream. *Int. J. Food Sci. Technol. Nutr*, *3*(1–2), 73–83.

Porto, B. C., Tribst, A. A. L., & Cristianini, M. (2018). Dynamic High Pressure Effects on Biopolymers: Polysaccharides and Proteins. In *Biopolymers for Food Design* (pp. 313–350). Elsevier. https://doi.org/10.1016/B978-0-12-811449-0.00010-4

Rojas, M. L., Leite, T. S., Cristianini, M., Alvim, I. D., & Augusto, P. E. D. (2016). Peach juice processed by the

ultrasound technology: Changes in its microstructure improve its physical properties and stability. *Food Research International*. https://doi.org/10.1016/j.foodres.2016.01.011

Shalaby, A. (2013). Antioxidant compounds, assays of determination and mode of action. *African Journal of Pharmacy and Pharmacology*, *7*(10), 528–539. https://doi.org/10.5897/AJPP2013.3474

Sharma, H., Singh, A. K., Deshwal, G. K., Rao, P. S., & Kumar, M. D. (2021). Functional Tinospora cordifolia (giloy) based pasteurized goat milk beverage: Impact of milk protein-polyphenol interaction on bioactive compounds, anti-oxidant activity and microstructure. *Food Bioscience*. https://doi.org/10.1016/j.fbio.2021.101101

Shukla, A., Goud, V. V., & Das, C. (2019). Antioxidant potential and nutritional compositions of selected ginger varieties found in Northeast India. *Industrial Crops and Products*. https://doi.org/10.1016/j.indcrop.2018.10.086

Singleton, V. L., Orthofer, R., & Lamuela-Raventós, R. M. (1999). [14] Analysis of total phenols and other oxidation substrates and antioxidants by means of folin-ciocalteu reagent. In *Methods in Enzymology* (pp. 152–178). https://doi.org/10.1016/S0076-6879(99)99017-1

Song, X., Zhou, C., Fu, F., Chen, Z., & Wu, Q. (2013). Effect of high-pressure homogenization on particle size and film properties of soy protein isolate. *Industrial Crops and Products*. https://doi.org/10.1016/j.indcrop.2012.08.005

Srinivasan, K. (2017). Ginger rhizomes (Zingiber officinale): A spice with multiple health beneficial potentials. *PharmaNutrition*, *5*(1), 18–28. https://doi.org/10.1016/j.phanu.2017.01.001

Suhag, R., Dhiman, A., Prabhakar, P. K., Sharma, A., Singh, A., & Upadhyay, A. (2022). Microfluidization of liquid egg yolk: Modelling of rheological characteristics and interpretation of flow behavior under a pipe flow. *Innovative Food Science & Emerging Technologies*, *81*, 103119. https://doi.org/10.1016/j.ifset.2022.103119

Suhag, R., Dhiman, A., Thakur, D., Kumar, A., & Upadhyay, A. (2021). Physico-chemical and functional properties of microfluidized egg yolk. *Journal of Food Engineering*, *294*, 110416. https://doi.org/10.1016/j.jfoodeng.2020.110416

Taghavi, E., Mirhosseini, H., Rukayadi, Y., Radu, S., & Biabanikhankahdani, R. (2018). Effect of Microfluidization Condition on Physicochemical Properties and Inhibitory Activity of Nanoemulsion Loaded with Natural Antibacterial Mixture. *Food and Bioprocess Technology*. https://doi.org/10.1007/s11947-017-2037-6

Tanweer, S., Mehmood, T., Zainab, S., Ahmad, Z., & Shehzad, A. (2020). Comparison and HPLC quantification of antioxidant profiling of ginger rhizome, leaves and flower extracts. *Clinical Phytoscience*, *6*(1), 12. https://doi.org/10.1186/s40816-020-00158-z

Tarafdar, A., & Kaur, B. P. (2021). Microfluidization-Driven Changes in Some Physicochemical Characteristics, Metal/Mineral Composition, and Sensory Attributes of Sugarcane Juice. *Journal of Food Quality*. https://doi.org/10.1155/2021/3326302

Tarafdar, A., Kaur, B. P., & Pareek, S. (2021). Effect of Microfluidization on Deteriorative Enzymes, Sugars, Chlorophyll, and Color of Sugarcane Juice. *Food and Bioprocess Technology*, *14*(7), 1375–1385. https://doi.org/10.1007/s11947-021-02651-w

Tarafdar, A., Kumar, Y., Kaur, B. P., & Badgujar, P. C. (2021). High-pressure microfluidization of sugarcane juice: Effect on total phenols, total flavonoids, antioxidant activity, and microbiological quality. *Journal of Food Processing and Preservation*, (March), 1–10. https://doi.org/10.1111/jfpp.15428

Tarafdar, A., Nair, S. G., & Pal Kaur, B. (2019). Identification of Microfluidization Processing Conditions for Quality Retention of Sugarcane Juice Using Genetic Algorithm. *Food and Bioprocess Technology*, *12*(11), 1874–1886. https://doi.org/10.1007/s11947-019-02345-4

Wang, X. M., Zhu, X. M., Zhang, N. H., Tu, Z. C., Wang, H., Liu, G. X., & Ye, Y. H. (2018). Morphological and structural characteristics of rice amylose by dynamic high-pressure microfluidization modification. *Journal of Food Processing and Preservation*. https://doi.org/10.1111/jfpp.13764

Wang, X., Wang, S., Wang, W., Ge, Z., Zhang, L., Li, C., et al. (2019). Comparison of the effects of dynamic high-pressure microfluidization and conventional homogenization on the quality of peach juice. *Journal of the Science of Food and Agriculture*. https://doi.org/10.1002/jsfa.9874

Yamaguchi, K., Kato, T., Noma, S., Igura, N., & Shimoda, M. (2010). The effects of high hydrostatic pressure treatment on the flavor and color of grated ginger. *Bioscience, Biotechnology and Biochemistry*. https://doi.org/10.1271/bbb.90712

Zhong, Z., Ming, W., & Feng, L. I. (2017). Effect of ginger juice on fermentative properties of yoghurt. *URL http://en. cnki. com. cn/Article_en/cjfdtotal-rylg200506007. htm. Accessed*, *6*.